



AALBORG UNIVERSITY
DENMARK

Aalborg Universitet

Layered Double Hydroxides for phosphorus recovery from acidified and non-acidified dewatered sludge

Lundehøj, Laura; Jensen, Henriette Casper; Wybrandt, Lisbeth; Nielsen, Ulla Gro; Christensen, Morten Lykkegaard; Quist-Jensen, Cejna Anna

Published in:
Water Research

DOI (link to publication from Publisher):
[10.1016/j.watres.2019.01.004](https://doi.org/10.1016/j.watres.2019.01.004)

Creative Commons License
CC BY-NC-ND 4.0

Publication date:
2019

Document Version
Accepted author manuscript, peer reviewed version

[Link to publication from Aalborg University](#)

Citation for published version (APA):

Lundehøj, L., Jensen, H. C., Wybrandt, L., Nielsen, U. G., Christensen, M. L., & Quist-Jensen, C. A. (2019). Layered Double Hydroxides for phosphorus recovery from acidified and non-acidified dewatered sludge. *Water Research*, 153, 208-216. Article 153. <https://doi.org/10.1016/j.watres.2019.01.004>

General rights

Copyright and moral rights for the publications made accessible in the public portal are retained by the authors and/or other copyright owners and it is a condition of accessing publications that users recognise and abide by the legal requirements associated with these rights.

- Users may download and print one copy of any publication from the public portal for the purpose of private study or research.
- You may not further distribute the material or use it for any profit-making activity or commercial gain
- You may freely distribute the URL identifying the publication in the public portal -

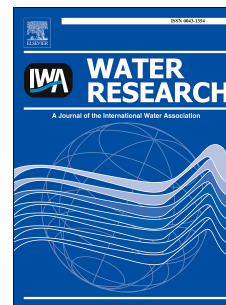
Take down policy

If you believe that this document breaches copyright please contact us at vbn@aub.aau.dk providing details, and we will remove access to the work immediately and investigate your claim.

Accepted Manuscript

Layered Double Hydroxides for phosphorus recovery from acidified and non-acidified dewatered sludge

L. Lundehøj, H.C. Jensen, L. Wybrandt, U.G. Nielsen, M.L. Christensen, C.A. Quist-Jensen



PII: S0043-1354(19)30031-4

DOI: <https://doi.org/10.1016/j.watres.2019.01.004>

Reference: WR 14369

To appear in: *Water Research*

Received Date: 19 October 2018

Revised Date: 7 January 2019

Accepted Date: 8 January 2019

Please cite this article as: Lundehøj, L., Jensen, H.C., Wybrandt, L., Nielsen, U.G., Christensen, M.L., Quist-Jensen, C.A., Layered Double Hydroxides for phosphorus recovery from acidified and non-acidified dewatered sludge, *Water Research*, <https://doi.org/10.1016/j.watres.2019.01.004>.

This is a PDF file of an unedited manuscript that has been accepted for publication. As a service to our customers we are providing this early version of the manuscript. The manuscript will undergo copyediting, typesetting, and review of the resulting proof before it is published in its final form. Please note that during the production process errors may be discovered which could affect the content, and all legal disclaimers that apply to the journal pertain.

Layered Double Hydroxides for phosphorus recovery from acidified and non-acidified dewatered sludge

L. Lundehøj¹, H.C. Jensen², L. Wybrandt², U. G. Nielsen¹, M.L. Christensen², C. A. Quist-Jensen^{2*}

¹ Department of Physics, Chemistry and Pharmacy, University of Southern Denmark, Campusvej 55, 5230 Odense M, Denmark

² Department of Chemistry and Bioscience, Aalborg University, Fredrik Bajers Vej 7H, 9220 Aalborg East, Denmark

* Author to whom correspondence should be addressed: cejna@bio.aau.dk

Abstract

Phosphate, which contains the essential element phosphorous (P), is a necessary fertilizer for agriculture, but the current phosphate deposits are running out and alternative sources are needed. Sludge obtained from wastewater treatment plants contains high concentrations of phosphorus and represents an alternative, sustainable source. In this study, sludge obtained from a wastewater treatment plant with biological and chemical phosphorus removal was acidified (pH = 3, 4, 5 and 6) to release orthophosphate followed by sequestration of the orthophosphate by a zinc aluminum layered double hydroxide (Zn₂Al-LDH). Sulfuric acid (H₂SO₄), nitric acid (HNO₃), and hydrochloric acid (HCl) was tested, which showed that only sulfate anions compete with phosphate and results in reduced phosphate recovery (25-35%). The orthophosphate concentration in the liquid phase increased from 20 % (raw sludge) to 75 % of the total phosphorus concentration at a pH of 3, which enhanced the phosphate uptake by the ZnAl-LDH from 1.7±0.2% to 60.3±0.6%. During acidification, the competing anion carbonate is degassed as CO₂, which further improved the phosphate uptake. PXRD showed the intercalation of carbonate in the LDH in the raw sludge at pH = 8, whereas orthophosphate was intercalated at lower pH values. ²⁷Al MAS NMR spectroscopy and powder X-ray diffraction (PXRD) proved preservation of the LDH at all pH values. Furthermore, about a third of the Al is present as an amorphous aluminum phosphate (AlPO₄) upon exposure to phosphate at low pH (pH = 3 and

26 5) based on ^{27}Al MAS NMR spectroscopy. At a pH of 6 about a third of the P is present as brushite
27 $(\text{CaHPO}_4 \cdot 2\text{H}_2\text{O})$.

28 **Keywords:** Layered Double Hydroxides (LDH), phosphate recovery, sludge acidification, wastewater, solid
29 state NMR Spectroscopy, ion exchange

30

31 **1.0 Introduction**

32 Phosphorus in the form of phosphate is an essential fertilizer in the agriculture and its supply in adequate
33 quantities is vital (Cordell et al., 2009; Shu et al., 2006). However, phosphate rock, a main source of
34 phosphate for fertilizers, is a critical resource (European Commission, 2018). Hence, research in alternative
35 phosphate sources, such as recovery of phosphate from wastewater, is demanded. The majority of the
36 phosphate at wastewater treatment plants is present in the sludge, mainly in the microbial mass or as
37 insoluble inorganic salts due to the biological and chemical removal of phosphate from the liquid phase,
38 respectively. Biological and/or chemical treatment procedures are necessary to meet the discharge limit set
39 by political regulations (de-Bashan and Bashan, 2004). Phosphate recovery/recycling by controlled
40 precipitation of struvite and calcium phosphate precipitation, which remove phosphate from the liquid phase
41 after sludge dewatering, do not exploit the full potential for phosphate recovery (Liu and Qu, 2017; Song et
42 al., 2006; Vasenko and Qu, 2017). Thus, the sludge contains valuable phosphate, but the direct application of
43 sludge to fields is problematic as toxins such as heavy metals, microplastic, and pathogens may be present in
44 critical quantities. Therefore, application of sludge on farmland has been banned in several European
45 countries (Milieu Ltd., 2010; Tarayrea et al., 2016). Incineration of sludge is an alternative, however the
46 bioavailability of the phosphorus is low and impurities from heavy metals is problematic for more than half
47 the ashes (Herzel et al., 2016). Furthermore, the method for heavy metal removal is expensive and the
48 sustainability of phosphorus recovery from ashes has been questioned (Vaneckhaute et al., 2017).

49 Recent studies have shown that the amount of phosphate in the liquid sludge phase is increased by
50 acidification due to dissolution of the inorganic phosphates in the sludge (Latif et al., 2015; Sun et al., 2012;

51 Wu et al., 2009). Antakyali et al. reported 75 % dissolution of phosphate from digested sewage sludge by
52 sludge acidification (Antakyali et al., 2013). Moreover, acidification improves the dewaterability of sludge
53 (Chen et al., 2001). Incineration after acidification is the best option, which simultaneously produces energy
54 (Lundin et al., 2004) as many European countries have banned the use of sludge in agriculture (Tarayrea et
55 al., 2016). However, sludge acidification also dissolves other metal salts and thereby releases heavy metals
56 bound in the sludge (Quist-Jensen et al., 2018; Wozniak and Huang, 1982). Thus, a selective phosphate
57 adsorbent for collecting of the released phosphate is needed.

58 Layered double hydroxides (LDHs) are considered promising adsorbents due to their high affinity for
59 orthophosphate (Cheng et al., 2009; Das et al., 2006; Yang et al., 2014), which are already manufactured on
60 an industrial scale. LDHs are anion exchange materials composed of positively charged layers of divalent
61 and trivalent cations octahedrally coordinated to edge sharing hydroxyl groups with anions (A) and water
62 intercalated between the layers in order to obtain a neutral charge (Figure 1). The general formula for an
63 LDH is $[M^{2+}_{1-x}M^{3+}_x(OH)_2]^{x+}(A^{n-}_{x/n}) \cdot yH_2O$, where M represents cations. A variety of anions, A, can be
64 intercalated and be exchanged for other anions in aqueous solutions giving LDHs their unique anion
65 exchange properties (Evans and Slade, 2006).

66 Phosphate adsorption by LDHs has been extensively tested in e.g. aqueous solutions (Ashekuzzaman and
67 Jiang, 2014; Das et al., 2006; He et al., 2010; Kuzawa et al., 2006; Yang et al., 2014), sewage sludge filtrate
68 (Cheng et al., 2009), seawater (Chitrakar et al., 2005), and waste water (Drenkova-Tuhtan et al., 2013). In
69 addition, the recyclability of the LDH by desorption of phosphate by a basic NaOH solution and subsequent
70 regeneration by calcination has been performed for MgFe and ZnAl LDHs for six to seven cycles
71 (Ashekuzzaman and Jiang, 2017; Cheng et al., 2009).

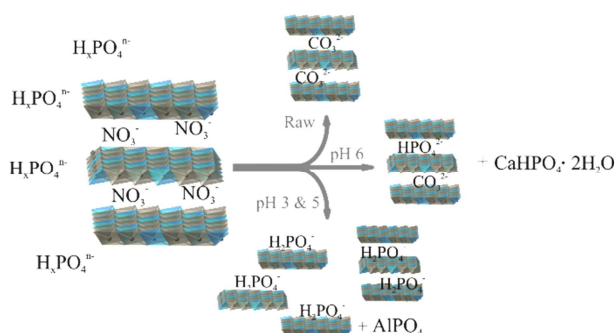
72 Alternatively, the phosphate incorporated in the LDH can be directly used as a fertilizer (Bernardo et al.,
73 2018; Everaert et al., 2016) or recovered by desorption (Chitrakar et al., 2005; He et al., 2010; Zhang et al.,
74 2016) followed by precipitation of as a calcium phosphate and regeneration of the LDH (Kuzawa et al.,
75 2006). The phosphate adsorption by ZnAl LDHs was nearly unchanged after five cycles (He et al., 2010).

76 Different implementations methods for LDHs based sorbents at wastewater treatment plants have been
 77 investigated. Direct addition of the solid LDHs provides a large surface area and is simple, but it is difficult
 78 to separate the LDH later (Goh et al., 2008). This can be circumvented by coating the LDH on magnetic
 79 materials and thereby perform magnetic separation after phosphate capture (Drenkova-Tuhtan et al., 2013) or
 80 by anchoring the LDH on a filter material or in membranes (Jia et al., 2018; Zhang et al., 2016).

81 Two of the major challenges for the design of the most efficient LDH sorbent are to understand how the
 82 LDHs capture P and the effect of competing anions. The most commonly studied LDH are MgAl, MgFe,
 83 CaAl, CaFe, and ZnAl LDH due to their limited toxicity and easy preparation. It is known that the
 84 hydrocalumites (CaAl and CaFe LDH), which have a slightly different crystal structure (Taylor, 1973), are
 85 destroyed upon phosphate exposure and calcium phosphates are formed (Radha et al., 2005; Xu et al., 2010).

86 Phosphate capture by the hydrotalcite LDHs including MgFe, ZnAl, and MgAl may proceed by both
 87 precipitation of phosphates (dissolution of the LDH) (Bernardo et al., 2016; Du et al., 2009; Radha et al.,
 88 2005) as well as intercalation, surface complexation and the pH dependence (Bernardo et al., 2016; Du et al.,
 89 2009; He et al., 2010; Radha et al., 2005; Yang et al., 2014).

90 Given the high affinity of LDH for especially phosphate and carbonate (Goh et al., 2008) both the pH
 91 dependent orthophosphate and the carbonate equilibria (Eqs. 1 to 6) are expected to affect the phosphate
 92 adsorption under variable pH conditions. At low pH, carbonate is degassed as CO_2 and will not compete with
 93 phosphate (Eqs 1-3). Above this pH carbonate is present mainly as HCO_3^- and competition is likely. Thus, an
 94 increase in the phosphate adsorption by the LDH is expected at low pH. The protonation of phosphate, which
 95 increases with pH, also affects the capacity.

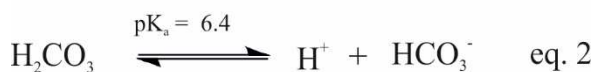


96

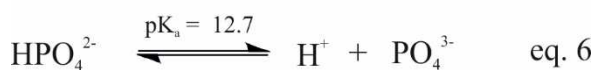
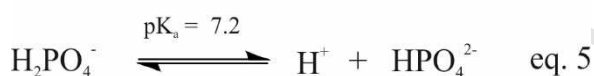
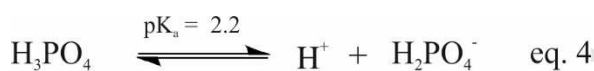
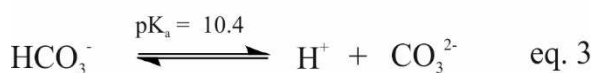
97

Figure 1: Illustration of layered double hydroxide (LDH) used for phosphorus recovery.

98



99



100

101 Phosphate is mainly present as HPO_4^{2-} in the pH range from 7.4 to 10.4, whereas phosphate mainly exist as
 102 H_2PO_4^- in the region between 2.2 and 7.4. Therefore, the phosphate adsorption is expected to be larger under
 103 acidic conditions due to the lower charge of phosphate anion. The objective of this study is to dissolve the
 104 orthophosphate bound in the sludge and investigate how the pH, spanning from untreated sludge and sludge
 105 acidified to a pH of 3, 5 and 6, respectively affects phosphate adsorption by a ZnAl LDH. Furthermore,
 106 competition from other anions, e.g., carbonate in the wastewater and the anion (nitrate, chloride, and sulfate)
 107 from the acid used for acidification, the stability of the LDH and the phosphate speciation after capture is
 108 also studied. This was addressed by performing adsorption studies followed by collecting of the solid
 109 product, which was characterized by powder X-ray diffraction (PXRD), ^{27}Al and ^{31}P MAS NMR
 110 spectroscopy. PXRD provide information about the crystalline phases and possible phosphate intercalation in
 111 the LDH, whereas ^{27}Al and ^{31}P MAS NMR give detailed insight into the stability of the LDH and phosphate
 112 speciation, respectively.

113 The ZnAl LDH was chosen over MgFe and MgAl LDHs for this study, as it has a high affinity for phosphate
 114 (He et al., 2010). MgFe LDHs are difficult to characterize by NMR due to the paramagnetic iron. For MgAl
 115 LDH precise quantification of the LDH content is difficult due to overlap of the ^{27}Al resonances from the

116 MgAl LDH and amorphous Al impurities (Pushparaj et al., 2015). Moreover, hydrothermal treatment of the
117 synthesis mixture was performed to reduce the amount of aluminum hydroxide (Pushparaj et al., 2015),
118 which is well known to bind phosphate (Emmerik et al., 2007; Li et al., 2013; Lookman et al., 1997).

119

120 **2.0 Materials and methods**

121 *2.1 Sludge characteristics*

122 Sludge was obtained from Aalborg West wastewater treatment plant (330.000 PE), Aalborg, Denmark. This
123 plant uses mainly biological treatment, but with potential addition of iron chloride as chemical treatment
124 after the aeration tanks. The sludge used in this study was obtained from the thermophilic digester (operating
125 at 55 °C), where excess sludge from the secondary treatment and primary sludge is added. The pH of the
126 sludge was adjusted by addition of 2M H₂SO₄, 2M HCl, or 7M HNO₃, respectively to the desired pH (3, 4, 5
127 and 6). The orthophosphate (o-P) and total-phosphate (t-P) were measured for each pH value according to
128 the procedure given in Danish Standards (Danish Standard, 1985a, 1985b). All analyses were performed in
129 triplicates. The samples were centrifuged at 5000 G in 10 minutes and filtered through a 15 µm filter before
130 o-P analysis and LDH addition. The dry matter content of the sludge was estimated by leaving around 15 g
131 of raw sludge in a drying oven at 105 °C for 24 hours. Afterwards, the dry matter was incinerated at 550 °C
132 for 2 h to determine the organic/inorganic matter. The pH and conductivity were measured using a Mettler
133 Toledo Seven Multi with a pH electrode BlueLine 17 (SI Analytics) and an Inlab 731 conductivity electrode
134 (Mettler Toledo). The ammonium concentration was measured by using the Berthelot method where
135 salicylate was used as a substitute for phenol (Danish Standard, 1975; Searle, 1984).

136 The concentration of cations in the raw sludge was measured on a inductively coupled plasma spectrometer
137 (ICP). First, the cations were extracted from sludge by concentrated HNO₃ and then the samples were filtered
138 through a 0.45-µm filter. The concentrations of Fe, Ca, Cr, Cu, Fe, Mg, Pb, and Zn were then quantified
139 using ICP (iCap 6300 DUO; Thermo Scientific, Waltham, MA, USA). The samples were measured in radial
140 view. 1 ppm Yttrium was used as the internal standard. All ICP measurements were made in duplicates.

141 Arsenic was measured by a test kit (Hach). NH_4^+ and cations have only been measured once, thus these
 142 values represent the sludge at the sampling time (April 2017). A detailed composition of the sludge can be
 143 found in Table 1. Notice that the metals in Table 1 are dissolved metals or metals bound to particles smaller
 144 than $0.45 \mu\text{m}$.

145 *Table 1: Chemical composition of sludge from the Aalborg West treatment plant.*

Composition		
pH	8.14 ± 0.57	-
t-P	1580.4 ± 21.4	mg/L
o-P	347.7 ± 65.4	mg/L
NH_4^+	1520.8	mg/L
Al	0.986	mg/L
Ca	10.9	mg/L
Cr	0.391	mg/L
Cu	0.122	mg/L
Fe	7.28	mg/L
Mg	2.73	mg/L
Pb	0.0114	mg/L
Zn	0.469	mg/L
As	< 0.2	mg/L
Dry matter	35.1 ± 0.7	g/kg
Organic matter	21.6 ± 0.5	g/kg
Inorganic matter	13.9 ± 0.6	g/kg

146

147

148 2.2 LDH synthesis

149 A $\text{Zn}_2\text{Al-LDH}$ (ideally $\text{Zn}_{0.66}\text{Al}_{0.33}(\text{OH})_2(\text{NO}_3)_{0.33} \cdot 2\text{H}_2\text{O}$) was utilized for phosphate recovery. The LDH was
 150 synthesized by co-precipitation at constant pH 8.5 followed by hydrothermal treatment, which gives the

151 highest purity LDH (Pushparaj et al., 2015). A solution with 0.67 M $\text{Zn}(\text{NO}_3)_2 \cdot 6\text{H}_2\text{O}$ and 0.33 M
152 $\text{Al}(\text{NO}_3)_3 \cdot 9\text{H}_2\text{O}$ (Zn:Al ratio of 2:1, total metal concentration 1 M) and a 1 M NaOH solutions were prepared
153 in decarbonated MiliQ water. The decarbonated water was produced by boiling the water and bubbling
154 nitrogen (N_2) through for at least 30 min. A N_2 was also bubbled through the reaction mixture as well to
155 minimize carbonate contamination. The reaction mixture was transferred to a hydrothermal bomb and placed
156 in the oven at 120 °C for 24h. The precipitated solid was washed three times with decarbonated MiliQ water
157 and collected by centrifugation before it was dried at 60 °C overnight. The sample was characterized by ICP-
158 EOS, powder X-ray diffraction, and solid state ^{27}Al MAS NMR spectroscopy. ICP-EOS showed a Zn:Al
159 ratio of 2.16. No non-LDH reflection was observed in the PXRD diffractograms, but analysis of the ^{27}Al
160 MAS NMR spectrum (Figure S1) showed that 15 ± 4 % of the Al in an amorphous aluminum hydroxide
161 phase (AOH) (Jensen et al., 2016; Pushparaj et al., 2015). Hence, the Zn:Al ratio of the LDH phase is
162 estimated to 2.54 based on ^{27}Al MAS NMR.

163

164 2.3 LDH adsorption

165 LDH adsorption studies were performed at ambient temperature at different pH values and LDH dosage. The
166 dosage of the LDH below pH of 7.2 was 0.882 g LDH/0.2 g o-P. At pH above 7.2 the dosage was doubled
167 (1.78 g LDH/0.2 g o-P) to account for changes in protonation (H_2PO_4^- vs HPO_4^{2-}). The LDH was dosed to 10
168 ml of sludge samples according to measured o-P concentration (triplicates). The samples were mixed using a
169 rotator mixer. After a given time, LDH was separated from solution by centrifugation at 5000 G for 5
170 minutes. o-P was analyzed in the solution before and after LDH adsorption (Triple analysis). The samples
171 were collected and dried at 60 °C overnight prior to PXRD and solid state NMR analyses. The adsorption
172 capacity ($C_{\%}$) was estimated from eq. 7.

173

$$C_{\%} = \frac{C_0 - C_t}{C_0} \cdot 100 \quad (\text{eq. 7})$$

174 where C_0 and C_t are the o-P concentration in the liquid phase before and after LDH adsorption, respectively.

175

176 *2.4 LDH characterization*

177 The PXRD diffractograms were collected on a Rigaku miniflex 600 with a Cu K- α radiation, a tube voltage
178 and current at 40 kV and 15 mA, respectively. The spectra were collected with a step size of 0.02° and a
179 speed of 10°/min in the 2 θ range from 5 to 70°.

180 Quantitative solid state ^{27}Al and ^{31}P MAS NMR spectra were recorded on a JEOL 500 MHz NMR
181 spectrometer using a 3.2 mm double resonance probe and a spinning speed of 13 kHz. The single pulse ^{27}Al
182 MAS NMR spectra were recorded with a relaxation delay of 1 s and short 10° pulse to ensure quantitative
183 spectra. A relaxation delay of 150 s was used for the single pulse ^{31}P MAS NMR spectra. The ^{31}P MAS
184 NMR spectra were analyzed using MestreNova.

185

186 **3.0 Results**

187 The phosphate release during acidification and phosphate adsorption by LDH using different acids are
188 discussed in the following section. Finally, LDH has been characterized after phosphorus adsorption to
189 determine how phosphorus adsorbs to LDH and if the LDH can sustain at a low pH.

190 *3.1 Acidification of sludge*

191 The sludge was acidified and the concentration of t-P and o-P were measured before and after centrifugation,
192 respectively (Figure 2). The pH was increased slightly after centrifugation due to removal of carbon dioxide,
193 but the maximum increase was 0.5 (pH 6). The concentration of o-P increased from about 300 mg/L (raw
194 sludge) to about 1200 mg/L (at pH 3) due to solution of inorganic phosphates, i.e., a fourfold increase in the
195 o-P concentration. 1200 mg/L corresponds to 75% to the total amount of phosphorus in the sludge, as
196 reported earlier (Antakyali et al., 2013).

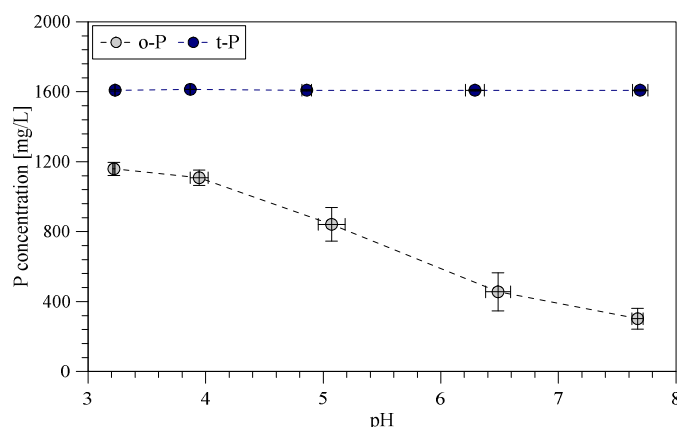


Figure 2: o-P and t-P concentration as a function of the sludge pH. Acidification was done by addition of 2M H_2SO_4

197

198

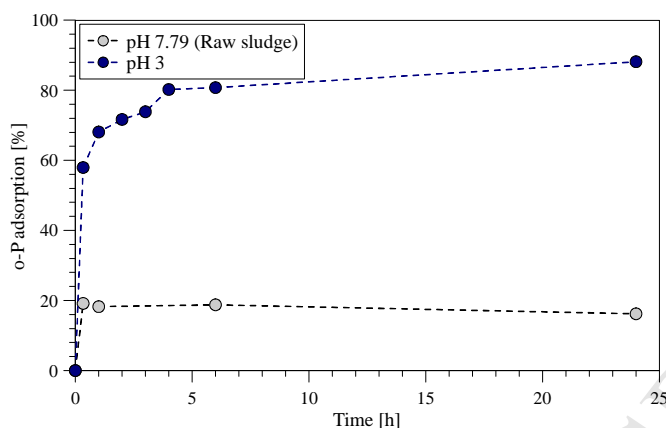
199

200 3.2 LDH uptake kinetics

201 The efficiency of o-P adsorption by of the ZnAl LDH was studied through the uptake kinetics. The LDH
 202 used in this study has incorporated NO_3^- as the negative ion and therefore, the sludge was only acidified with
 203 HNO_3 in the kinetic studies to avoid competition with other anions.

204 Around 90% of the o-P in the liquid phase is adsorbed in sludge acidified to pH 3 and only around 20 % in
 205 the raw sludge (pH 7.79). At the highest pH, the adsorption kinetics stabilizes after 20 minutes, whereas for a
 206 pH of 3 the amount of o-P adsorbed increased from 57.9 ± 0.6 % at 20 minutes to 80.2 ± 2.2 % after 4 hours
 207 (Figure 3). The reason for the poor adsorption at higher pH was most probably due to competition with
 208 carbonate at near neutral pH, whereas less carbonate is present at low pH due to CO_2 degassing (vide infra).
 209 The CO_2 degassing is also observed from the buffer capacity of the sludge (c.f., Figure S2 in supplementary
 210 information including the experimental method to obtain the buffer capacity). The phosphate equilibrium
 211 was taken into account in the kinetics studies, as described in section 2.3.

212



213

214 *Figure 3: Kinetics of phosphate adsorption at different pH. $[o-P]_{initial}=229.3\pm 11.9$ mg/L at pH 7.79 and $[o-P]_{initial}=1157.1\pm 25.2$*
 215 *mg/L at pH 3.*

216

217 The zinc concentrations in the aqueous phases were measured by ICP before and after adsorption probe if the
 218 LDH is partially dissolved, as illustrated in Table 2 for the kinetic studies using nitric acid. The LDH is
 219 maintained in the raw sludge since the Zn concentration corresponds to less than one percent. However,
 220 about 8-10 % of the Zn is dissolved at a pH of 3 . To further test the conservation of LDH at low pH,
 221 analysis of the solid phase LDHs are reported in section 3.4.

222

Table 2: Zn concentration in solution after LDH dosage.

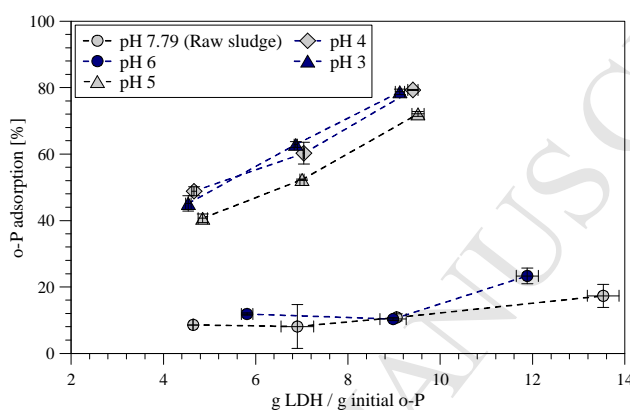
Time [h]	Raw sludge		pH 3	
	Zn [mg/L] after adsorption	Zn released [%]	Zn [mg/L] after adsorption	Zn released [%]
1	8.23	0.291	230	8.13
6	10.3	0.371	245	8.82
24	6.96	0.249	303	10.8

223

224 3.3 Phosphate adsorption at different pH

225 Phosphate adsorption was evaluated at five different pH values (pH = 3, 4, 5, 6, 7.79 (raw sludge)), where
 226 the pH was adjusted by addition of HNO₃ prior to addition of different amounts of LDH (Figure 4). A small
 227 increase in the pH of approx. 0.5 ± 0.2 was always observed immediately after addition of LDH due to its

228 basic nature. Similarly, the adsorption increased when the pH was lower, but it is evident that there is a gap
 229 between pH 5 and pH 6, c.f., Figure 4. The phosphate adsorption increases from 10.2 ± 1.6 % to 44.9 ± 3.3 %
 230 at dosage of 4-6g LDH/g o-P due to the favorable shift in the carbonate equilibrium as CO_2 is degassing
 231 during acidification (vide supra). It was also noted that higher LDH amount results in an improved phosphate
 232 adsorption. However, the increase at high pH (from 8-10% to 16-24%) was limited compared to the lower
 233 pH (from 40-50% to 72-80%). Therefore, addition of more LDH was more favorable at low pH.



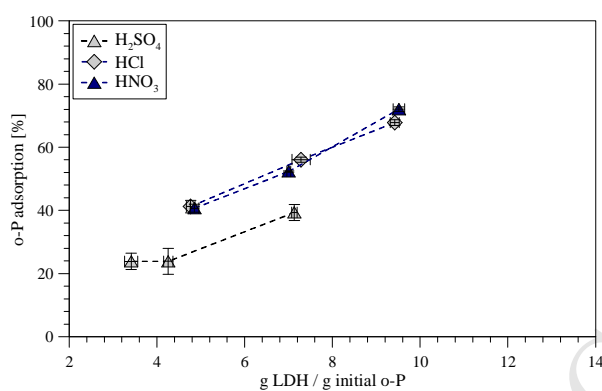
234

235 *Figure 4: Adsorption of o-P using HNO_3 . Adsorption time: 2h. $[\text{o-P}]_{\text{initial}}$ was 1229.1, 1086.6, 743.0, 360.1, 254.1 mg/L for pH 3, 4,
 236 5, 6 and 7.79, respectively*

237

238 Three different acids (HCl , HNO_3 and H_2SO_4) were used to acidify the digested sludge to pH 5 and 3.
 239 Subsequently, the phosphate adsorption was measured after addition of various amounts of LDH (Figure 5).
 240 Similar amount of o-P was adsorbed for sludge acidified with HCl and HNO_3 indicating that Cl^- and NO_3^-
 241 did not influence the adsorption significantly. However, a significant reduction of the phosphate adsorption
 242 was seen for sulfate. For example, only 39.4 ± 2.5 % of the phosphate was adsorbed on the LDH at a pH of 5
 243 when sulfuric acid was used as compared to 55.2 ± 0.9 % for nitric and hydrochloric acid at 7.2 g LDH/g o-P.
 244 This indicates that sulfate ions compete with phosphate to bind in LDH, as also observed in other studies on
 245 phosphate adsorption (Das et al., 2006; Halajnia et al., 2013). The o-P concentration in the liquid phase
 246 increased from about 20 % in the raw sludge to 75 % at pH 3 with respect to the t-P concentration. Thus the
 247 total phosphorus recovery increases significantly by acidification. For example, acidification by HNO_3
 248 results in total phosphorus recovery of 60.3 ± 0.6 % at a pH of 3, which was much higher than obtained for the

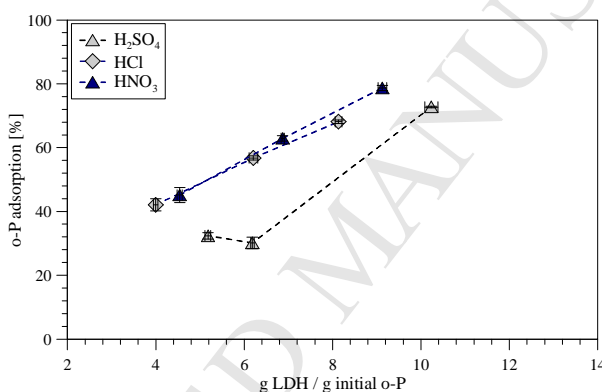
249 raw sludge ($1.7 \pm 0.2\%$). This illustrates that high o-P concentrations, which may be achieved by acidification
 250 or other techniques, may be required for an efficient recovery by LDH.



251

252

(a)



253

254

(b)

255 *Figure 5: Adsorption of o-P at (a) pH 5 ($[o-P]_{initial}$ was 825.8, 812.6 and 743.0 mg/L for H₂SO₄, HCl and HNO₃, respectively), and*
 256 *(b) pH 3 ($[o-P]_{initial}$ was 1258.0, 1235.7 and 1229.0 mg/L for H₂SO₄, HCl and HNO₃, respectively). Adsorption time: 2h.*

257

258 3.4 Characterization of the solid phases after adsorption

259 The solid phase was collected after exposure of the LDH to the different sludge samples and subsequently
 260 characterization by a combination of PXRD, ²⁷Al and ³¹P MAS NMR spectroscopy, which provided
 261 information about both the crystalline and amorphous samples as well as the stability of the LDH at the
 262 different pH values.

263

264 3.4.1 PXRD

265 For LDH, the basal (003) and (006) reflections in the PXRD diffractograms (Figure 6) are related to the
266 interlayer distances and are consequently a signature of the intercalated anion. The (003) reflection as well as
267 the predominant reflections from non-LDH phases are summarized in Table 2. A ZnAl-LDH phase is
268 observed for all samples, but there are significant changes in the intercalated anion and crystallinity of the
269 LDH. A substantial decrease in the crystallinity of the LDH after exposure to sludge is evident as a
270 broadening of the reflections and their decreased intensity. However, the characteristic (110) reflection from
271 the LDH is present in all the samples. It is related to a ($a = 2d(110)$) of the unit cell for the LDH and thereby
272 the metal-metal distance in the layers. Thus, the LDH structure is preserved even at a pH of 3.

273 For the raw sludge sample (pH = 8.14) the position of the basal reflections corresponds to the intercalation of
274 carbonate (Liu and Yang, 2016), which shift to lower 2θ values (larger interlayer spacing) at a pH of 6
275 matching those reported for LDH intercalated with HPO_4^{2-} (Costantino et al., 1997). The (003) reflection at
276 this pH is very broad and span values for carbonate and hydrogen phosphates as well as overlaps with a
277 reflection from brushite ($\text{CaHPO}_4 \cdot 2\text{H}_2\text{O}$) (Figure 6c). Thus, LDH intercalated with HPO_4^{2-} and CO_3^{2-} may
278 coexist at a pH of 6. The basal reflections shift to even lower 2θ values at pH of 5 corresponds to the
279 intercalation of H_2PO_4^- , which also results in a third reflection at $2\theta = 22.4^\circ$, as reported earlier (Costantino et
280 al., 1997) (Figure 6d). The increased phosphate uptake at the lower pH values is favored by a combination of
281 the phosphate protonation and degassing of carbonate (Eqs. 1-6).

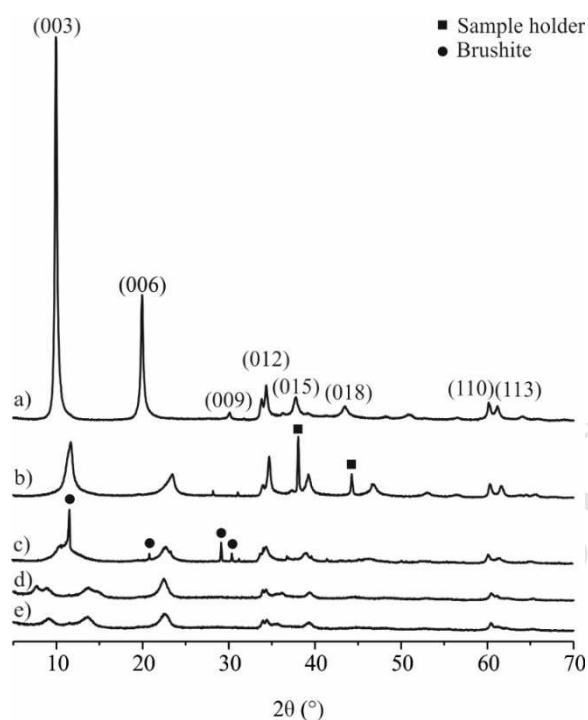
282 The PXRD diffractograms of the pH of 5 and 3 samples contain three similar reflections in the $5\text{-}30^\circ$ range
283 (Figures 6d and 6e). The reflection with the lowest 2θ value (8.9° at pH of 5 and 9.1° at of pH 3) does not
284 match the interlayer spacing of an LDH intercalated with a common, small inorganic anion such as NO_3^- ,
285 CO_3^{2-} , SO_4^{2-} , Cl^- , or HPO_4^{2-} (Costantino et al., 1997; Liu and Yang, 2016; Tang et al., 2008). However, it is
286 close to the reported value for the (003) reflection for ZnAl-LDH intercalated with formate (HCOO^-)
287 (Costantino et al., 1997), pyrophosphate ($\text{P}_2\text{O}_7^{4-}$) and triphosphate ($\text{P}_3\text{O}_{10}^{5-}$) (Badreddine et al., 1999).
288 Nevertheless, the expected (006) reflection is not observed (Figure 6d and 6e). Hence, intercalation of
289 formate, pyrophosphate, or triphosphate does not seem likely. The possible lack of the (00 l) reflections

290 indicate that the layers must be disrupted. The two others partially match iron dihydrogen phosphate
 291 ($\text{Fe}(\text{H}_2\text{PO}_4)_3$) (ICSD 162423) and vivianite ($\text{Fe}_2(\text{PO}_4)_3 \cdot 8\text{H}_2\text{O}$) (ICSD 30645) in agreement with the high Fe
 292 content in the sludge (7.28 mg/L), c.f., Table 1, but further analysis was not possible. The pH = 6 sample
 293 contains brushite ($\text{CaHPO}_4 \cdot 2\text{H}_2\text{O}$) and two weak reflections of unknown origin are observed for the raw
 294 sample (Table 3 and Figure 6b). Thus, the increase in the phosphate uptake as compared to the raw sample is
 295 caused by a combination of HPO_4^{2-} intercalation and the precipitation of brushite (Figure 6). A minor
 296 reflection from brushite is visible in the diffractogram for the samples with a pH of 5 and 3 as well, but no
 297 resonance for brushite is observed in the ^{31}P MAS NMR spectra of these samples. Hence, if present the
 298 concentration is most likely less than 5 % of the total P. Precipitation of brushite and its solubility is
 299 dependent on temperature, concentration and pH (Ferreira et al., 2003; Lundager Madsen and Thorvardarson,
 300 1984).

301 *Table 3. The position of the interlayer reflections, (003) and from the LDH with the predominant intercalated anion in the crystalline*
 302 *phases listed. Furthermore, the most intense reflections from other phases and their assignment, when possible, is given.*

Sample	(003)	LDH Anion	Other reflections	Assignment
Precursor	10.0°	NO_3^-		
Raw	11.6°	CO_3^{2-}	28.2° and 31.2°	Unknown
pH 6	10.8° (broad)	HPO_4^{2-} and CO_3^{2-}	11.6°, 20.9°, 29.2°, 20.4°, 31.3°	$\text{CaHPO}_4 \cdot 2\text{H}_2\text{O}$
pH 5	7.7°	H_2PO_4^-	9.1° 13.4° and 22.4°	Unknown Unknown
pH 3			8.9° 13.4° and 22.4°	Unknown Unknown

303



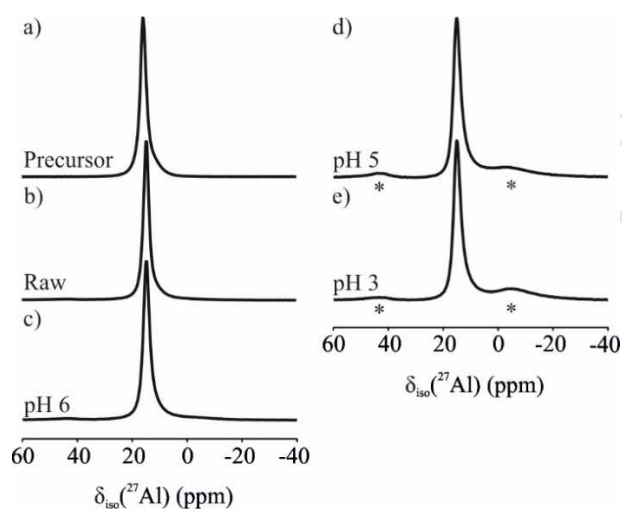
304

305 *Figure 6. PXRD for a) The precursor: Zn_2Al-NO_3 LDH, b) Zn_2Al-NO_3 exposed to raw sludge. Reflections from the sample holder are*
 306 *seen in the sample. c) Zn_2Al-NO_3 exposed to sludge at pH 6, d) Zn_2Al-NO_3 exposed to sludge at pH 5. d) Zn_2Al-NO_3 exposed to sludge*
 307 *at pH 3.*

308 3.4.2 ^{27}Al MAS NMR spectroscopy

309 The ^{27}Al MAS NMR spectra (Figure 7) provided information about the stability of the LDH structure and
 310 other phases as well as information about amorphous Al containing phases. The resonance from a Zn_2Al-
 311 LDH is seen for all samples implying at least partial preservation of the LDH structure. However, non-LDH
 312 resonances are also present at a pH of 5 and 3 and to a minor extent at a pH of 6 indicating that some of the
 313 LDH is transformed to a new aluminum containing phase. These two new, broad ^{27}Al resonances located in
 314 the region for tetrahedral and octahedral aluminum at $\delta(^{27}Al) \approx 44$ ppm and -5 ppm, respectively (Figures 7d
 315 and 7e). These values match those reported in studies of amorphous aluminum phosphates precipitated under
 316 similar pH conditions (pH = 3-7.5). The resonance located at 44 ppm was assigned to tetrahedrally
 317 coordinated aluminum to phosphate whereas the resonance at -5 ppm was assigned to octahedrally
 318 aluminum coordinated to phosphate or to four phosphate and two hydroxyl/water ligands (Burrell et al.,

319 2001; Lookman et al., 1997). Hence, it can be concluded that part of the LDH converts, e.g., by dissolution-
 320 reprecipitation, into amorphous aluminum phosphate, which constitute approx. 20-25% of the Al in the
 321 sample at a pH of 3 (Figure 6). A full dissolution of the LDH does not occur due to the basicity of LDHs. It
 322 cannot be excluded that some of aluminum hydroxide as well is converted to aluminum phosphate upon
 323 exposure to phosphate at low pH values (Lookman et al., 1997).



324

325 *Figure 7. ^{27}Al MAS NMR spectra for the a) precursor $\text{Zn}_2\text{Al-NO}_3$, $\text{Zn}_2\text{Al-NO}_3$ exposed to b) raw sludge, c) sludge at pH 6, d) sludge
 326 at pH 5, and e) sludge at pH 3. * Indicates the amorphous aluminum phosphate (see discussion in text).*

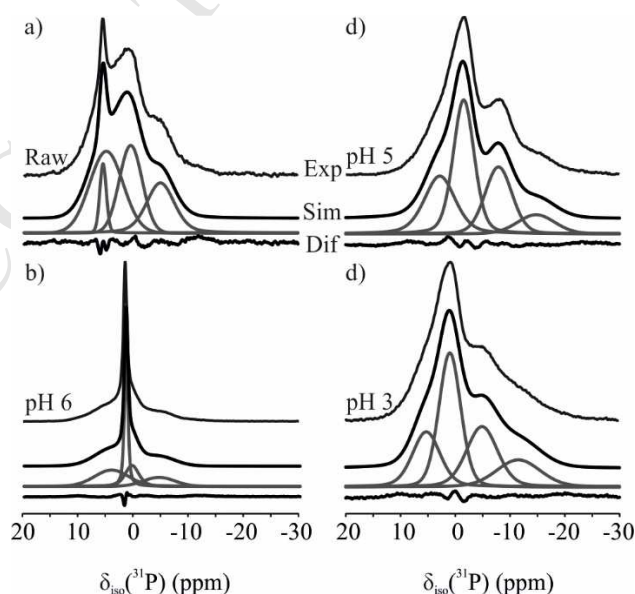
327

328 3.4.3 ^{31}P MAS NMR spectroscopy.

329 ^{31}P MAS NMR spectra were recorded of all the samples to identify and quantify the different phosphate
 330 species present. The isotropic chemical shift (δ_{iso}) and intensity obtained from deconvolution of the spectra
 331 in Figure 8 are summarized in Table 4. One signal is observed in all the spectra, accompanied by one to two
 332 weak set of spinning side band (ssb) for the raw, pH 5, and pH 3 samples and sharper ssbs for the pH 6
 333 sample due to a narrow resonance. The three resonances at $\delta_{\text{iso}}(^{31}\text{P}) = 4.7(5)$ ppm, $\delta_{\text{iso}}(^{31}\text{P}) = 0.7(3)$ ppm and
 334 $\delta_{\text{iso}}(^{31}\text{P}) = -5(1)$ ppm are present in all the samples. PXRD and ^{27}Al MAS NMR show LDH and aluminum
 335 hydroxide to be the only phases present in all the samples, and hence the three resonances must therefore be
 336 from phosphate adsorbed to one of these materials. Earlier studies of phosphate adsorption on the closely
 337 related MgAl-LDH showed resonances approximately in the region 0 to 10 ppm based on visual inspection

338 of the ^{31}P MAS NMR spectra (Hou et al., 2003), whereas phosphate adsorbed on aluminum hydroxides are in
 339 the region 0 to -20 ppm (Emmerik et al., 2007; Li et al., 2013, 2010; Lookman et al., 1997). Thus, the first
 340 two resonances are assigned to the LDH phase. About 20 % of the sample is AOH so we tentatively assign
 341 the -5.0(1) ppm resonance to phosphate adsorbed to the AOH phase, but some of the phosphate may be
 342 associated with the LDH.

343 The resonance with $\delta_{\text{iso}}(^{31}\text{P}) \approx -11.4$ ppm is unambiguously present for the pH 5 and 3 sample, which are
 344 known to contain aluminum phosphates from ^{27}Al MAS NMR and the $\delta_{\text{iso}}(^{31}\text{P})$, and match those reported for
 345 amorphous aluminum phosphate (Lookman et al., 1997). Thus, ^{31}P MAS NMR confirms the precipitation of
 346 amorphous aluminum phosphate at the low pH values possibly due to a partial dissolution of the LDH. The
 347 most intense resonance in the spectra for the sample with a pH of 6, which constitute 32 ± 3 % of the total
 348 intensity and has a $\delta_{\text{iso}}(^{31}\text{P}) = 1.5(2)$, is assigned to brushite based on earlier reported ^{31}P NMR data (Aue et
 349 al., 1984) and the PXRD (Figure 6). Brushite could not be unambiguously identified in the ^{31}P MAS NMR
 350 spectra at a pH of 5 and 3 due to overlap with other resonances, but it may be present in minor quantities (< 5
 351 %) as weak reflections from brushite are seen in the PXRD (Figure 6d and 6e). A sharp, well defined
 352 resonance with $\delta_{\text{iso}}(^{31}\text{P}) = 5.6(2)$ ppm and a relative concentration of 7 ± 3 % most likely result of another O-P
 353 mineral, which may be related to the unknown reflections in the PXRD (Figure 6b).



354
 355 *Figure 8. ^{31}P MAS NMR spectra of the $\text{Zn}_2\text{Al-NO}_3$ LDH to a) raw sludge, b) sludge at pH 6, c) sludge at pH 5 and d) sludge at pH 3.*

356

Table 4. The different P species identified and quantified from deconvolutions of the ^{31}P MAS NMR spectra in Figure 10.

Sample	Assignment	$\delta_{\text{iso}}(^{31}\text{P})$ (ppm)	I[%]
Raw	Unknown	5.6±2	7±3
	LDH-P	5.0±4	41±5
	LDH-P	0.6±3	30±5
	AOH-P	-4.9±3	22±5
pH 6	LDH-P	4.2±5	33±6
	Brushite	1.5±2	32±3
	LDH-P	0.5±5	18±5
	AOH-P	-4.5±5	17±6
pH 5	LDH-P	4.5±5	26±4
	LDH-P	0.6±3	40±6
	AOH-P	-5.1±4	25±6
	AlPO ₄	-11.3±5	10±4
pH 3	LDH-P	5.2±4	20±4
	LDH-P	1.0±3	39±6
	AOH-P	-4.9±5	25±5
	AlPO ₄	-11.5±5	15±4

357

358 Discussion

359 *Practical implementation*

360 Acidification is a known technology to improve dewaterability (Cai et al., 2018; Chen et al., 2001) and
 361 simultaneously dissolve orthophosphate (Antakyali et al., 2013; Quist-Jensen et al., 2018), which has been
 362 tested on both pilot and large scale applications (Antakyali et al., 2013; Cai et al., 2018). The acid
 363 consumption is higher for digested sludge compared to non-digest sludge due to the bicarbonate buffer
 364 system (CO₂ stripping) and an increased dissolution/release of phosphorus during acidification of the

365 digested sludge (Quist-Jensen et al., 2018). Mainly inorganic salts are being dissolved during acidification
366 (Latif et al., 2015; Sun et al., 2012; Wu et al., 2009). As a consequence, the phosphorus release depends on
367 whether phosphorus is removed biologically and/or chemically at the WWTP. In this study, acidification of
368 the sludge was performed using three different acids to investigate how this affects phosphorus adsorption by
369 LDH. Sulfate competes with phosphate leading to a reduced phosphate uptake, whereas chloride and nitrate
370 did not influence this. Other anions such as arsenate could potentially also compete with o-P, however, LDH
371 has a slightly higher affinity for phosphate than arsenate (Violante et al., 2009). Competitive intercalation
372 have been observed especially at low pH (Goh et al., 2008; Violante et al., 2009; Wang et al., 2018).
373 Nevertheless, arsenate uptake by the LDH under our conditions is not likely given the extremely low
374 concentration of arsenic (0.2 mg/L - Table 1) as compared to that of o-P (approx. 347 mg/L).

375 Separation of the LDH from the liquid phase are not practical with the tested LDH particles. This highlights
376 the importance of developing magnetic separation of LDH (Drenkova-Tuhtan et al., 2013) or embedding
377 LDH in filter materials or membranes (Jia et al., 2018; Zhang et al., 2016).

378 *Preservation of the LDH*

379 LDHs are typically unstable below a pH of 4 (He et al., 2006), but our data clearly show that LDH is present
380 at all pH value also at pH 3. At pH = 5 and 3, AlPO_4 are present (approx. 20-25 % of the Al), which indicates
381 a partial dissolution of the LDH at these pH values in agreement with the increased $[\text{Zn}^{2+}]$ in the solution.
382 ICP result showed a 10.8 % release of Zn, hence the Al source for the precipitated AlPO_4 is a both the LDH,
383 the AOH and/or sludge. Most likely, the hydroxide released by partial dissolution of the LDH increases the
384 pH preventing further dissolution of the LDH.

385 *Phosphate speciation*

386 The phosphate uptake (o-P) is pH dependent and most efficient at low pH, primarily due to the favorable
387 shift in the carbonate equilibrium towards carbon dioxide below a pH of 6.4. In addition, the lower charge (-
388 1) of the o-P at low pH allow for a higher adsorption. Precipitation of 32 ± 3 % brushite (pH of 6) or 10-15 %
389 AlPO_4 (pH of 5 and 3) is seen, which is ascribed to combination of a high Ca concentration (10.9 mg/l) in the
390 sludge (Table 1) and the appropriate pH. The precipitation of AlPO_4 cannot account for the increased

391 phosphate adsorption from 10.2 ± 1.6 % (pH 6) to 44.9 ± 3.3 % (pH 5). Precipitation of iron phosphates has
392 been observed after MgFe LDH was exposed to phosphate at a pH of 5 (Du et al., 2009), but often
393 precipitation of the appropriate magnesium or zinc phosphates are seen at a pH higher than 5 (Bernardo et
394 al., 2016; Radha et al., 2005; Seftel et al., 2018). It is also found that 17-25 % of the adsorbed phosphate is
395 adsorbed to the AOH phase, an impurity in the LDH sample, which thereby is a large contributor to
396 phosphate uptake. The result indicates the presence of two different binding sites, e.g., intercalated and
397 surface adsorbed phosphate. However, further studies are needed to assign these to different LDH sites and
398 will be reported elsewhere.

399

400 **4.0 Conclusion**

401 Up to 75% of the phosphorus was extracted from digested sludge by adding nitric, hydrochloric or sulfuric
402 acid. The solid material was removed and ZnAl-LDH added to adsorb the dissolved phosphate.

- 403 • The ZnAl-LDH phosphate binding capacity was favored at low pH by degassing of CO_2 and
404 protonation of phosphate to form H_2PO_4^- .
- 405 • Sulfated reduced phosphate binding; hence acidification by sulfuric acid resulted in the lowest
406 phosphate removal.
- 407 • LDH was mainly preserved at pH 3, but small part of the LDH was probably dissolved and
408 precipitated as a new aluminum phase
- 409 • Phosphate was both intercalated in LDH by ion-exchange and adsorption.

410 Thus, ZnAl-LDH selectively removed phosphate from acidified sludge, whereby phosphorus can be
411 recovered and the iron containing liquid recycled to the active sludge process to precipitate phosphate.

412

413 **Acknowledgement**

414 The Innovation Fund Denmark is gratefully acknowledged for partially funding this work through the project
415 “RecoverP” and the authors also gratefully acknowledge the partial funding from Ecoinnovation – MUDP
416 for the project “Genindvinding af fosfor fra spildevandsslam – mål: 80 % genindvinding af fosfor” (in
417 English: Recovery of phosphorus from wastewater sludge – target 80 % recovery of phosphorus). Financial
418 support from the Villum Foundation via the “Villum Young Investigator Programme” (grant
419 VKR022364; UGN, LL) and 600 MHz NMR (Villum Center for Bioanalytical Services) is greatly
420 appreciated. Ms Carina Lohman is thanked for the ICP-OES analyses. The authors thank Aalborg West
421 wastewater treatment plant for providing the sludge samples.

422

423 **References**

- 424 Antakyali, D., Meyer, C., Preyl, V., Maier, W., Steinmetz, H., 2013. Large-scale application of nutrient
425 recovery from digested sludge as struvite. *Water Pract. Technol.* 8, 256–262.
426 <https://doi.org/10.2166/wpt.2013.027>
- 427 Ashekuzzaman, S.M., Jiang, J.Q., 2017. Strategic phosphate removal/recovery by a re-usable Mg–Fe–Cl
428 layered double hydroxide. *Process Saf. Environ. Prot.* 107, 454–462.
429 <https://doi.org/10.1016/j.psep.2017.03.009>
- 430 Ashekuzzaman, S.M., Jiang, J.Q., 2014. Study on the sorption-desorption-regeneration performance of Ca-,
431 Mg- and CaMg-based layered double hydroxides for removing phosphate from water. *Chem. Eng. J.*
432 246, 97–105. <https://doi.org/10.1016/j.cej.2014.02.061>
- 433 Aue, W.P., Roufosse, A.H., Glimcher, M.J., Griffin, R.G., 1984. Solid-State Phosphorus-31 Nuclear
434 Magnetic Resonance Studies of Synthetic Solid Phases of Calcium Phosphate: Potential Models of
435 Bone Mineral. *Biochemistry* 23, 6110–6114. <https://doi.org/10.1021/bi00320a032>
- 436 Badreddine, M., Legrouri, A., Barroug, A., De Roy, A., Besse, J.P., 1999. Ion exchange of different
437 phosphate ions into the zinc–aluminium–chloride layered double hydroxide. *Mater. Lett.* 38, 391–395.
438 [https://doi.org/10.1016/S0167-577X\(98\)00195-5](https://doi.org/10.1016/S0167-577X(98)00195-5)

- 439 Bernardo, M.P., Guimarães, G.G.F., Majaron, V.F., Ribeiro, C., 2018. Controlled Release of Phosphate from
440 Layered Double Hydroxide Structures: Dynamics in Soil and Application as Smart Fertilizer. ACS
441 Sustain. Chem. Eng. 6, 5152–5161. <https://doi.org/10.1021/acssuschemeng.7b04806>
- 442 Bernardo, M.P., Moreira, F.K.V., Colnago, L.A., Ribeiro, C., 2016. Physico-chemical assessment of [Mg-Al-
443 PO₄]-LDHs obtained by structural reconstruction in high concentration of phosphate. Colloids Surfaces
444 A Physicochem. Eng. Asp. 497, 53–62. <https://doi.org/10.1016/j.colsurfa.2016.02.021>
- 445 Burrell, L.S., Johnston, C.T., Schulze, D., Klein, J., White, J.L., Hem, S.L., 2001. Aluminium phosphate
446 adjuvants prepared by precipitation at constant pH. Part I: composition and structure. Vaccine 19, 275–
447 281.
- 448 Cai, M.Q., Hu, J.Q., Wells, G., Seo, Y., Spinney, R., Ho, S.H., Dionysiou, D.D., Su, J., Xiao, R., Wei, Z.,
449 2018. Understanding Mechanisms of Synergy between Acidification and Ultrasound Treatments for
450 Activated Sludge Dewatering: From Bench to Pilot-Scale Investigation. Environ. Sci. Technol. 52,
451 4313–4323. <https://doi.org/10.1021/acs.est.8b00310>
- 452 Chen, Y., Yang, H., Gu, G., 2001. Effect of acid and surfactant treatment on activated sludge dewatering and
453 settling. Water Res. 35, 2615–2620. [https://doi.org/10.1016/S0043-1354\(00\)00565-0](https://doi.org/10.1016/S0043-1354(00)00565-0)
- 454 Cheng, X., Huang, X., Wang, X., Zhao, B., Chen, A., Sun, D., 2009. Phosphate adsorption from sewage
455 sludge filtrate using zinc–aluminum layered double hydroxides. J. Hazard. Mater. 169, 958–964.
456 <https://doi.org/10.1016/j.jhazmat.2009.04.052>
- 457 Chitrakar, R., Tezuka, S., Sonoda, A., Sakane, K., Ooi, K., Hirotsu, T., 2005. Adsorption of phosphate from
458 seawater on calcined MgMn-layered double hydroxides. J. Colloid Interface Sci. 290, 45–51.
459 <https://doi.org/10.1016/j.jcis.2005.04.025>
- 460 Cordell, D., Drangert, J.-O., White, S., 2009. The story of phosphorus: Global food security and food for
461 thought. Glob. Environ. Chang. 19, 292–305.
- 462 Costantino, U., Casciola, M., Massinelli, L., Nocchetti, M., Vivani, R., 1997. Intercalation and grafting of
463 hydrogen phosphates and phosphonates into synthetic hydrotalcites and a.c.-conductivity of the
464 compounds thereby obtained. Solid State Ionics 97, 203–212. [https://doi.org/10.1016/S0167-
465 2738\(97\)00043-X](https://doi.org/10.1016/S0167-2738(97)00043-X)

- 466 Danish Standard, 1985a. DS 291:1985.
- 467 Danish Standard, 1985b. DS 292:1985.
- 468 Danish Standard, 1975. DS 224:1975.
- 469 Das, J., Patra, B.S., Baliarsingh, N., Parida, K.M., 2006. Adsorption of phosphate by layered double
470 hydroxides in aqueous solutions. *Appl. Clay Sci.* 32, 252–260.
471 <https://doi.org/10.1016/j.clay.2006.02.005>
- 472 de-Bashan, L.E., Bashan, Y., 2004. Recent advances in removing phosphorus from wastewater and its future
473 use as fertilizer (1997–2003). *Water Res.* 38, 4222–4246. <https://doi.org/10.1016/j.watres.2004.07.014>
- 474 Drenkova-Tuhtan, A., Mandel, K., Paulus, A., Meyer, C., Hutter, F., Gellermann, C., Sextl, G., Franzreb, M.,
475 Steinmetz, H., 2013. Phosphate recovery from wastewater using engineered superparamagnetic
476 particles modified with layered double hydroxide ion exchangers. *Water Res.* 47, 5670–5677.
477 <https://doi.org/10.1016/j.watres.2013.06.039>
- 478 Du, Y., Rees, N., O’Hare, D., 2009. A study of phosphate absorption by magnesium iron hydroxycarbonate.
479 *Dalt. Trans.* 75, 8197–8202. <https://doi.org/10.1039/b909853d>
- 480 Emmerik, T.J. Van, Sandström, D.E., Antzutkin, O.N., Angove, M.J., Johnson, B.B., 2007. 31P Solid-State
481 Nuclear Magnetic Resonance Study of the Sorption of Phosphate onto Gibbsite and Kaolinite.
482 *Langmuir* 23, 3205–3213.
- 483 European Commission, 2018. Report on Critical Raw Materials and the Circular Economy.
- 484 Evans, D.G., Slade, R.C.T., 2006. Structural Aspects of Layered Double Hydroxides, in: Duan, X., Evans,
485 D.G. (Eds.), *Layered Double Hydroxides*. Springer Berlin Heidelberg, Berlin, Heidelberg, pp. 1–87.
486 https://doi.org/10.1007/430_005
- 487 Everaert, M., Warrinnier, R., Baken, S., Gustafsson, J.P., De Vos, D., Smolders, E., 2016. Phosphate-
488 Exchanged Mg-Al Layered Double Hydroxides: A New Slow Release Phosphate Fertilizer. *ACS*
489 *Sustain. Chem. Eng.* 4, 4280–4287. <https://doi.org/10.1021/acssuschemeng.6b00778>
- 490 Ferreira, A., Oliveira, C., Rocha, F., 2003. The different phases in the precipitation of dicalcium phosphate
491 dihydrate. *J. Cryst. Growth* 252, 599–611. [https://doi.org/10.1016/S0022-0248\(03\)00899-6](https://doi.org/10.1016/S0022-0248(03)00899-6)
- 492 Goh, K.-H., Lim, T.-T., Dong, Z., 2008. Application of layered double hydroxides for removal of oxyanions:

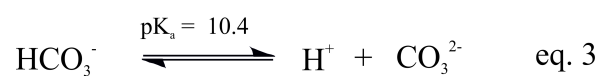
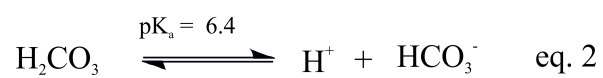
- 493 A review. *Water Res.* 42, 1343–1368. <https://doi.org/10.1016/J.WATRES.2007.10.043>
- 494 Halajnia, A., Oustan, S., Najafi, N., Khataee, A.R., Lakzian, A., 2013. Adsorption-desorption characteristics
495 of nitrate, phosphate and sulfate on Mg²⁺/Al layered double hydroxide. *Appl. Clay Sci.* 80–81, 305–312.
496 <https://doi.org/10.1016/j.clay.2013.05.002>
- 497 He, H., Kang, H., Ma, S., Bai, Y., Yang, X., 2010. High adsorption selectivity of ZnAl layered double
498 hydroxides and the calcined materials toward phosphate. *J. Colloid Interface Sci.* 343, 225–231.
499 <https://doi.org/10.1016/j.jcis.2009.11.004>
- 500 He, J., Wei, M., Li, B., Kang, Y., Evans, D.G., Duan, X., 2006. Preparation of Layered Double Hydroxides,
501 in: Duan, X., Evans, D.G. (Eds.), *Layered Double Hydroxides*. Springer Berlin Heidelberg, Berlin,
502 Heidelberg, pp. 89–119. https://doi.org/10.1007/430_006
- 503 Herzel, H., Krüger, O., Hermann, L., Adam, C., 2016. Sewage sludge ash — A promising secondary
504 phosphorus source for fertilizer production. *Sci. Total Environ.* 542, 1136–1143.
505 <https://doi.org/10.1016/j.scitotenv.2015.08.059>
- 506 Hou, X., Bish, D.L., Wang, S.-L., Johnston, C.T., Kirkpatrick, R.J., 2003. Hydration, expansion, structure,
507 and dynamics of layered double hydroxides. *Am. Mineral.* 88, 167–179.
- 508 Jensen, N.D., Bjerring, M., Nielsen, U.G., 2016. A solid state NMR study of layered double hydroxides
509 intercalated with para-amino salicylate, a tuberculosis drug. *Solid State Nucl. Magn. Reson.* 78, 9–15.
510 <https://doi.org/10.1016/j.ssnmr.2016.06.001>
- 511 Jia, Z., Hao, S., Lu, X., 2018. Exfoliated Mg–Al–Fe layered double hydroxides/polyether sulfone mixed
512 matrix membranes for adsorption of phosphate and fluoride from aqueous solutions. *J. Environ. Sci.*
513 (China) 70, 63–73. <https://doi.org/10.1016/j.jes.2017.11.012>
- 514 Kuzawa, K., Jung, Y.J., Kiso, Y., Yamada, T., Nagai, M., Lee, T.G., 2006. Phosphate removal and recovery
515 with a synthetic hydrotalcite as an adsorbent. *Chemosphere* 62, 45–52.
516 <https://doi.org/10.1016/j.chemosphere.2005.04.015>
- 517 Latif, M.A., Mehta, C.M., Batstone, D.J., 2015. Low pH anaerobic digestion of waste activated sludge for
518 enhanced phosphorous release. *Water Res.* 81, 288–293. <https://doi.org/10.1016/j.watres.2015.05.062>
- 519 Li, W., Feng, J., Kwon, K.D., Kubicki, J.D., Phillips, B.L., 2010. Surface Speciation of Phosphate on

- 520 Boehmite (γ -AlOOH) Determined from NMR Spectroscopy. *Langmuir* 26, 4753–4761.
521 <https://doi.org/10.1021/la903484m>
- 522 Li, W., Feng, X., Yan, Y., Sparks, D.L., Phillips, B.L., 2013. Solid-State NMR Spectroscopic Study of
523 Phosphate Sorption Mechanisms on Aluminum (Hydr)oxides. *Environ. Sci. Technol.* 47, 8308–8315.
524 <https://doi.org/10.1021/es400874s>
- 525 Liu, Y., Qu, H., 2017. Effects of Solution Composition and Polymer Additive on the Crystallization of
526 Struvite. *Chem. Eng. Technol.* 40, 1–8.
- 527 Liu, Y., Yang, Z., 2016. Intercalation of sulfate anions into a Zn–Al layered double hydroxide: their
528 synthesis and application in Zn–Ni secondary batteries. *RSC Adv.* 6, 68584–68591.
529 <https://doi.org/10.1039/C6RA09096F>
- 530 Lookman, R., Grobet, P., Merckx, R., Van Riemsdijk, W.H., 1997. Application of ^{31}P and ^{27}Al MAS NMR
531 for phosphate speciation studies in soil and aluminium hydroxides: promises and constraints. *Geoderma*
532 80, 369–388. [https://doi.org/10.1016/S0016-7061\(97\)00061-X](https://doi.org/10.1016/S0016-7061(97)00061-X)
- 533 Lundager Madsen, H.E., Thorvardarson, G., 1984. Precipitation of calcium phosphate from moderately acid
534 solution. *J. Cryst. Growth* 66, 369–376. [https://doi.org/10.1016/0022-0248\(84\)90220-3](https://doi.org/10.1016/0022-0248(84)90220-3)
- 535 Lundin, M., Olofsson, M., Pettersson, G.J., Zetterlund, H., 2004. Environmental and economic assessment of
536 sewage sludge handling options. *Resour. Conserv. Recycl.* 41, 255–278.
537 <https://doi.org/10.1016/j.resconrec.2003.10.006>
- 538 Milieu Ltd., 2010. Environmental, economic and social impacts of the use of sewage sludge on land Final
539 Report Part I: Overview Report.
- 540 Pushparaj, S.S.C., Forano, C., Prevot, V., Lipton, A.S., Rees, G.J., Hanna, J. V., Nielsen, U.G., 2015. How
541 the Method of Synthesis Governs the Local and Global Structure of Zinc Aluminum Layered Double
542 Hydroxides. *J. Phys. Chem. C* 119, 27695–27707. <https://doi.org/10.1021/acs.jpcc.5b09490>
- 543 Quist-Jensen, C.A., Wybrandt, L., Løkkegaard, H., Antonsen, S.B., Jensen, H.C., Nielsen, A.H., Christensen,
544 M.L., 2018. Acidification and recovery of phosphorus from digested and non-digested sludge. *Water*
545 *Res.* 146, 307–317.
- 546 Radha, A. V., Kamath, P.V., Shivakumara, C., 2005. Mechanism of the anion exchange reactions of the

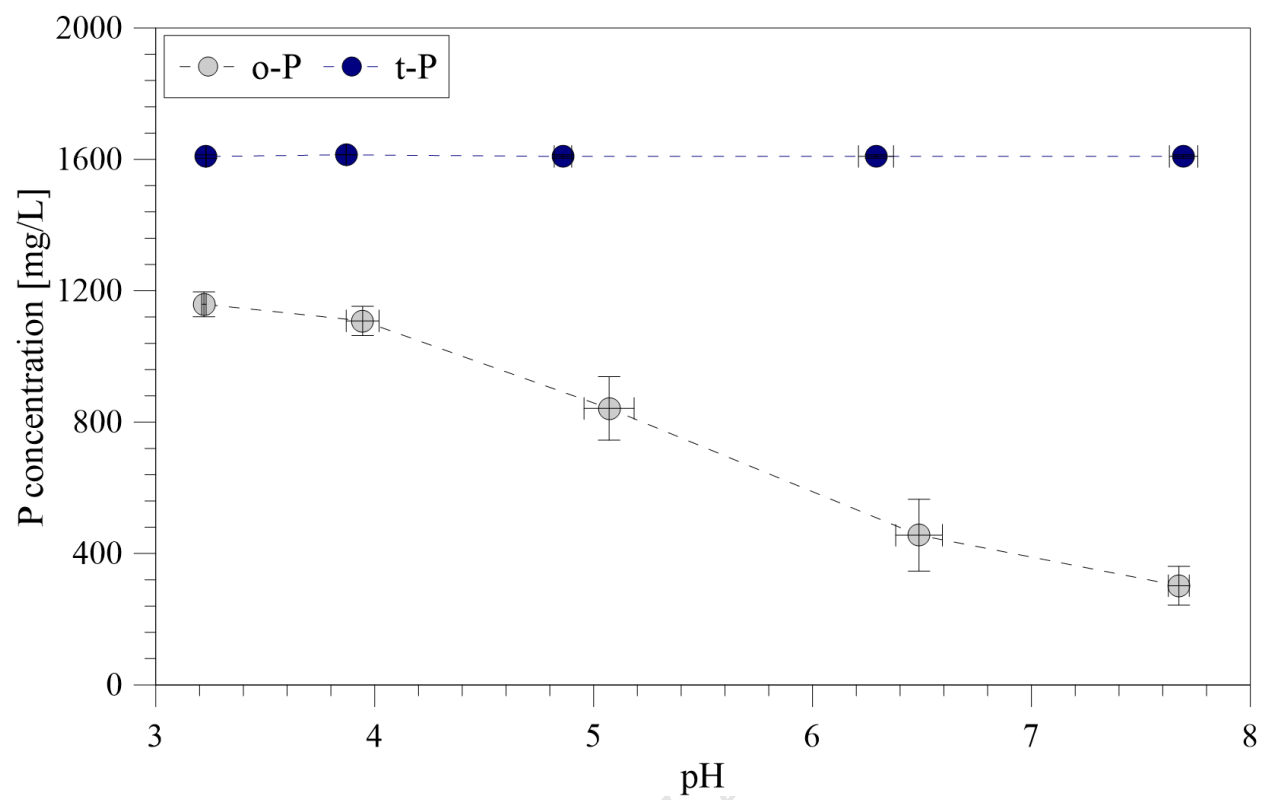
- 547 layered double hydroxides (LDHs) of Ca and Mg with Al. *Solid State Sci.* 7, 1180–1187.
548 <https://doi.org/10.1016/j.solidstatesciences.2005.05.004>
- 549 Searle, P.L., 1984. The berthelot or indophenol reaction and its use in the analytical chemistry of nitrogen: A
550 review. *Analyst* 109, 549–568. <https://doi.org/10.1039/AN9840900549>
- 551 Seftel, E.M., Ciocarlan, R.G., Michielsen, B., Meynen, V., Mullens, S., Cool, P., 2018. Insights into
552 phosphate adsorption behavior on structurally modified ZnAl layered double hydroxides. *Appl. Clay*
553 *Sci.* 165, 234–246. <https://doi.org/10.1016/j.clay.2018.08.018>
- 554 Shu, L., Schneider, P., Jegatheesan, V., Johnson, J., 2006. An economic evaluation of phosphorus recovery
555 as struvite from digester supernatant. *Bioresour. Technol.* 97, 2211–2216.
556 <https://doi.org/10.1016/j.biortech.2005.11.005>
- 557 Song, Y., Weidler, P.G., Berg, U., N?esch, R., Donnert, D., 2006. Calcite-seeded crystallization of calcium
558 phosphate for phosphorus recovery. *Chemosphere* 63, 236–243.
559 <https://doi.org/10.1016/j.chemosphere.2005.08.021>
- 560 Sun, X., Wang, W., Chen, C., Luo, C., Li, J., Shen, J., Wang, L., 2012. Acidification of Waste Activated
561 Sludge During Thermophilic Anaerobic Digestion. *Procedia Environ. Sci.* 16, 391–400.
562 <https://doi.org/10.1016/j.proenv.2012.10.055>
- 563 Tang, P., Xu, X., Lin, Y., Li, D., 2008. Enhancement of the thermo- and photostability of an anionic dye by
564 intercalation in a zinc-aluminum layered double hydroxide host. *Ind. Eng. Chem. Res.* 47, 2478–2483.
565 <https://doi.org/10.1021/ie0710420>
- 566 Tarayrea, C., Clercq, L. De, Charlier, R., Michels, E., Meers, E., Camargo-Valero, M., Delvigne, F., 2016.
567 New perspectives for the design of sustainable bioprocesses for phosphorus recovery from waste.
568 *Bioresour. Technol.* 206, 264–274. <https://doi.org/10.1016/J.BIORTECH.2016.01.091>
- 569 Taylor, H.F.W., 1973. Crystal structures of some double hydroxide minerals. *Mineral. Mag.* 39, 377–389.
570 <https://doi.org/10.1180/minmag.1973.039.304.01>
- 571 Vaneekhaute, C., Lebuf, V., Michels, E., Belia, E., Vanrolleghem, P.A., Tack, F.M.G., Meers, E., 2017.
572 Nutrient Recovery from Digestate: Systematic Technology Review and Product Classification. *Waste*
573 *and Biomass Valorization* 8, 21–40.

- 574 Vasenko, L., Qu, H., 2017. Effect of NH₄-N/P and Ca/P molar ratios on the reactive crystallization of
575 calcium phosphates for phosphorus recovery from wastewater. *J. Cryst. Growth* 459, 61–66.
- 576 Violante, A., Pucci, M., Cozzolino, V., Zhu, J., Pigna, M., 2009. Sorption/desorption of arsenate on/from
577 Mg-Al layered double hydroxides: Influence of phosphate. *J. Colloid Interface Sci.* 333, 63–70.
578 <https://doi.org/10.1016/j.jcis.2009.01.004>
- 579 Wang, J., Zhang, T., Li, M., Yang, Y., Lu, P., Ning, P., Wang, Q., 2018. Arsenic removal from
580 water/wastewater using layered double hydroxide derived adsorbents, a critical review. *RSC Adv.* 8,
581 22694–22709. <https://doi.org/10.1039/c8ra03647k>
- 582 Wozniak, D.J., Huang, J.Y.C., 1982. Variables affecting metal removal from sludge. *Water Pollut. Control*
583 *Fed.* 54, 1574–1580. <https://doi.org/10.2307/25041763>
- 584 Wu, H., Yang, D., Zhou, Q., Song, Z., 2009. The effect of pH on anaerobic fermentation of primary sludge at
585 room temperature. *J. Hazard. Mater.* 172, 196–201. <https://doi.org/10.1016/j.jhazmat.2009.06.146>
- 586 Xu, Y., Dai, Y., Zhou, J., Xu, Z.P., Qian, G., Lu, G.Q.M., 2010. Removal efficiency of arsenate and
587 phosphate from aqueous solution using layered double hydroxide materials: Intercalation vs.
588 precipitation. *J. Mater. Chem.* 20, 4684–4691. <https://doi.org/10.1039/b926239c>
- 589 Yang, K., Yan, L., Yang, Y., Yu, S., Shan, R., Yu, H., Zhu, B., Du, B., 2014. Adsorptive removal of
590 phosphate by Mg–Al and Zn–Al layered double hydroxides: Kinetics, isotherms and mechanisms. *Sep.*
591 *Purif. Technol.* 124, 36–42. <https://doi.org/10.1016/j.seppur.2013.12.042>
- 592 Zhang, X., Guo, L., Huang, H., Jiang, Y., Li, M., Leng, Y., 2016. Removal of phosphorus by the core-shell
593 bio-ceramic/Zn-layered double hydroxides (LDHs) composites for municipal wastewater treatment in
594 constructed rapid infiltration system. *Water Res.* 96, 280–291.
595 <https://doi.org/10.1016/j.watres.2016.03.063>

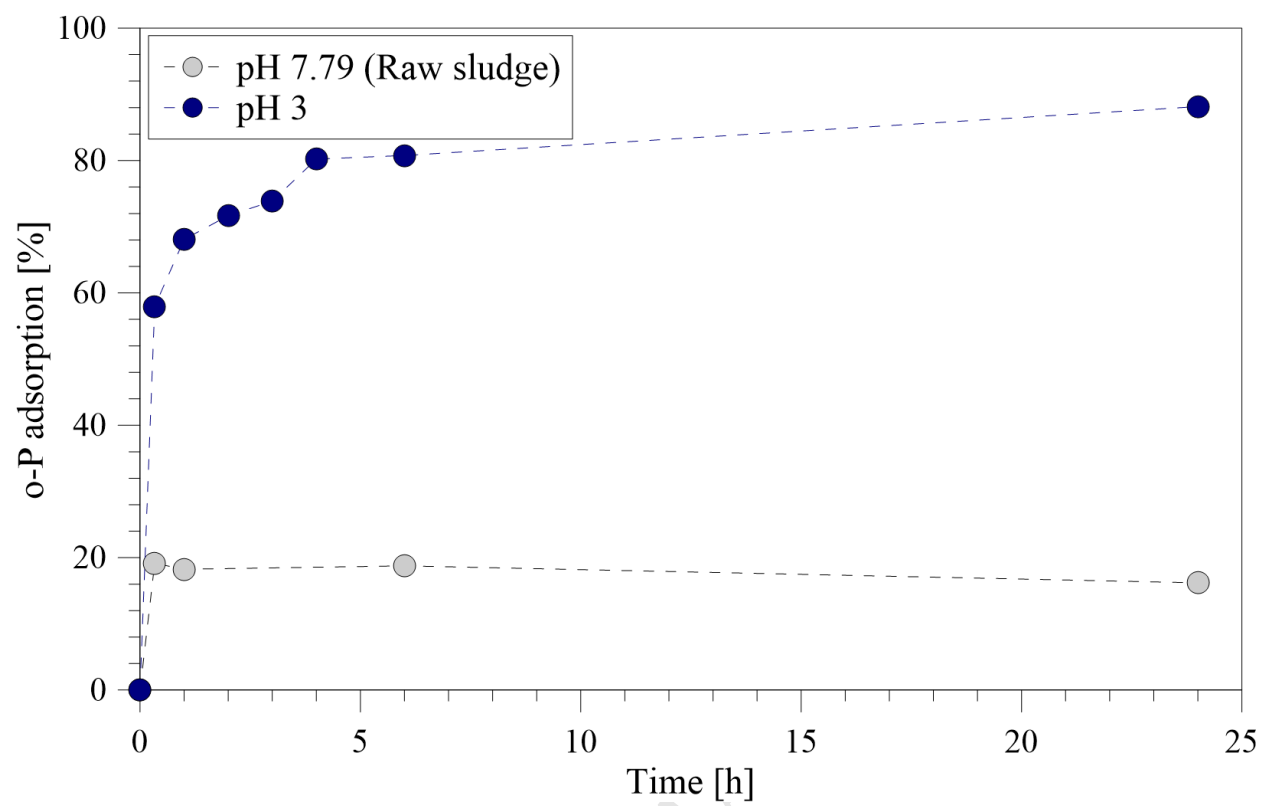
596

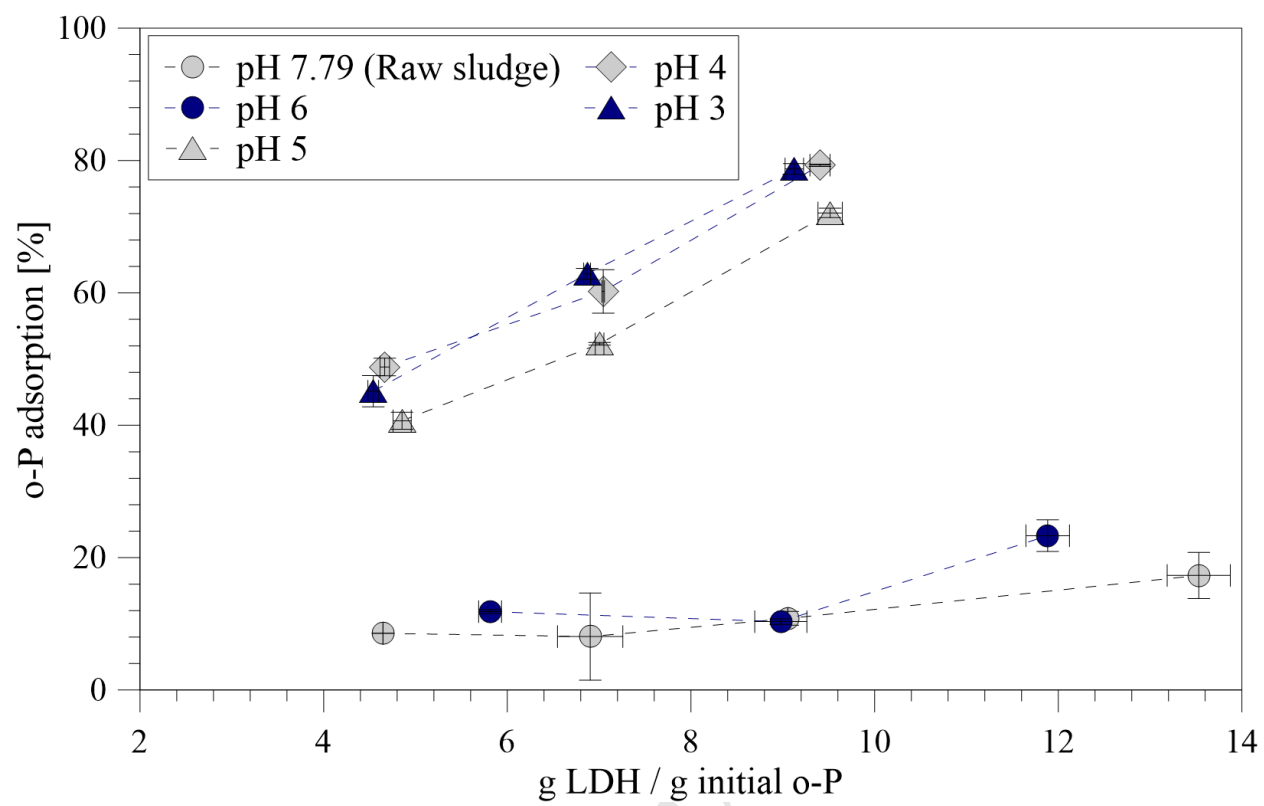


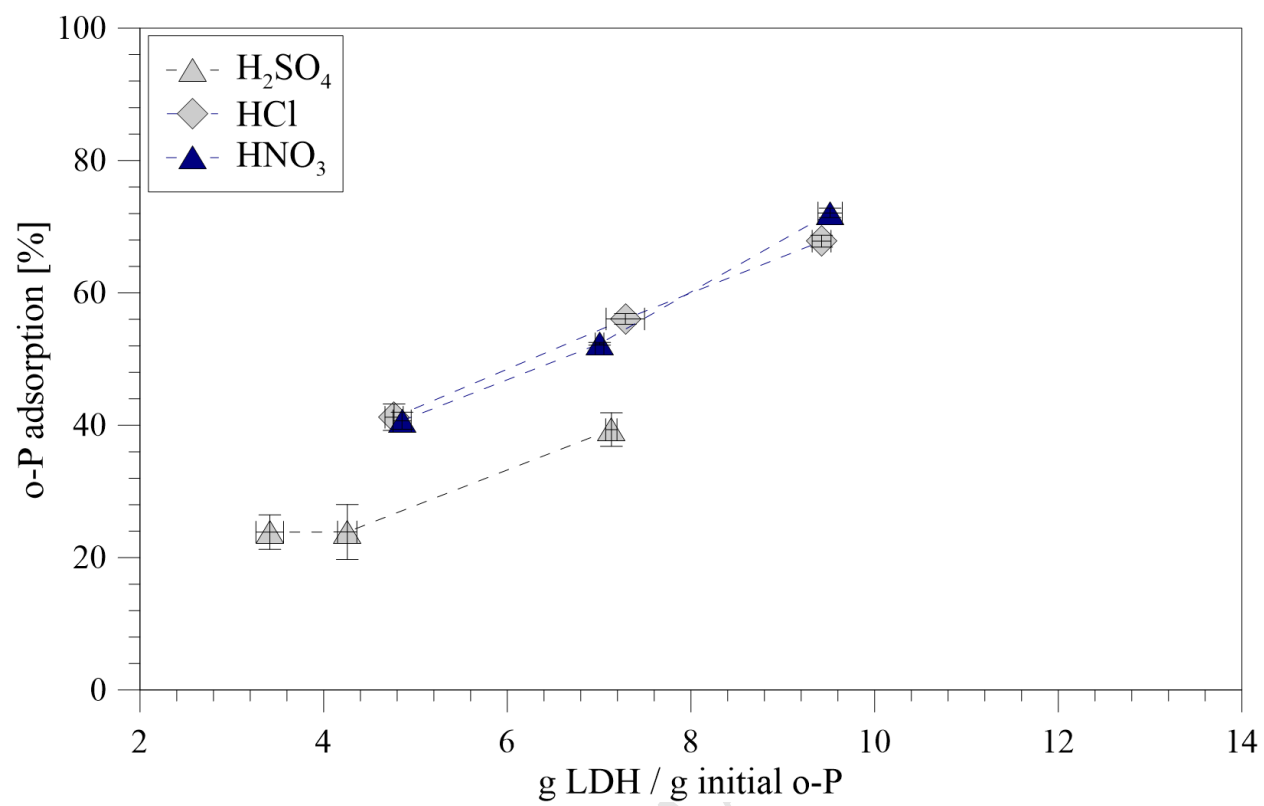
ACCEPTED MANUSCRIPT

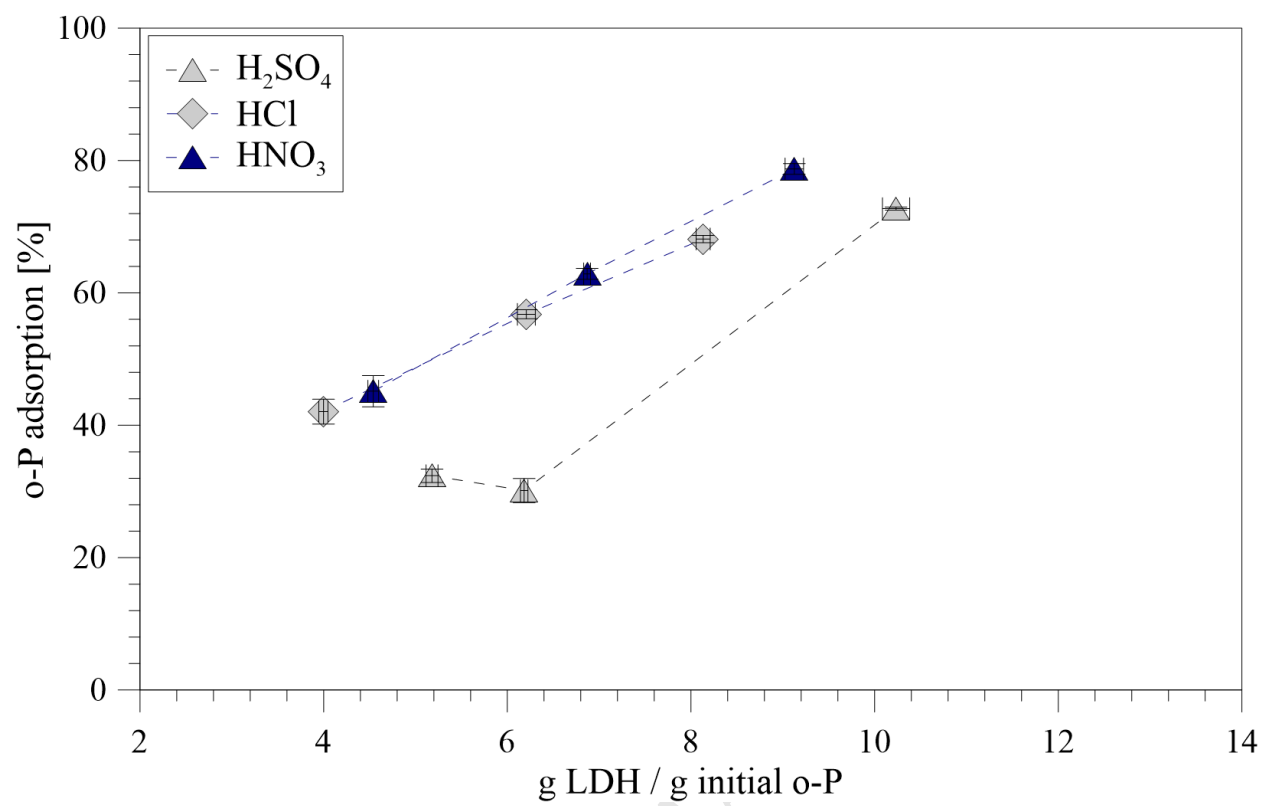


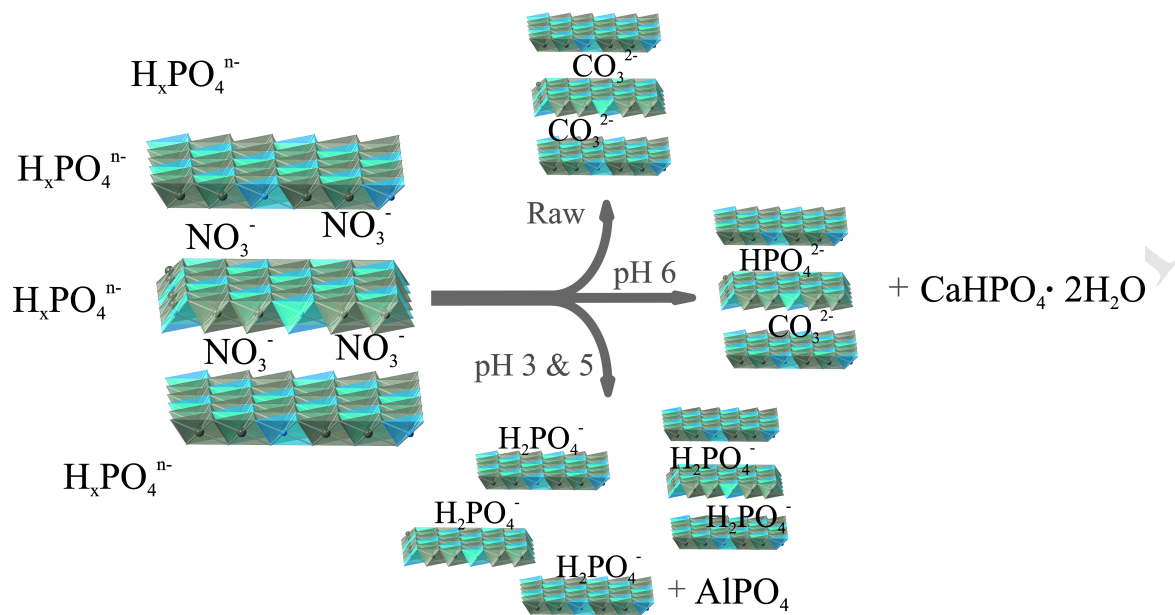
ACCEPTED MANUSCRIPT

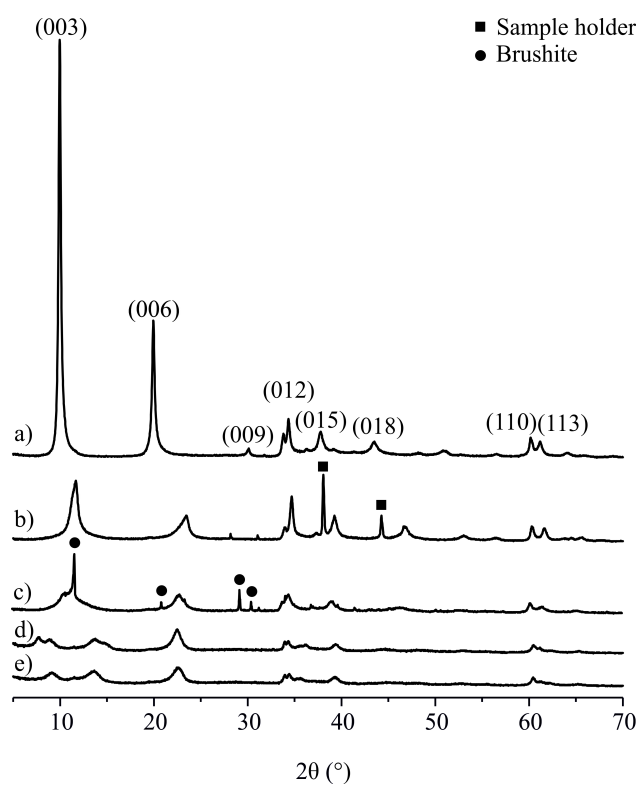


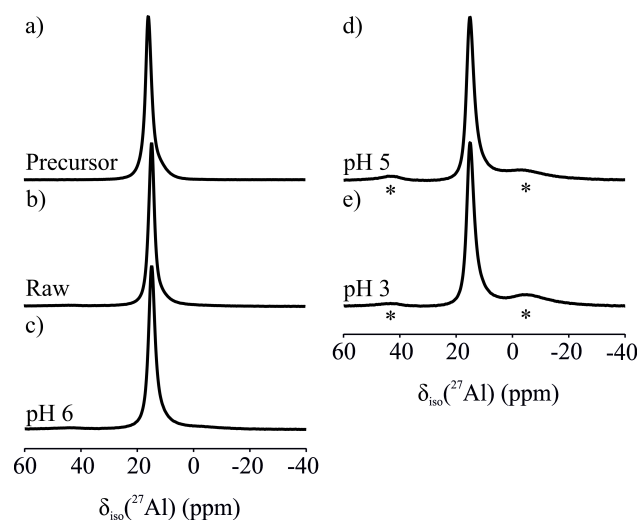


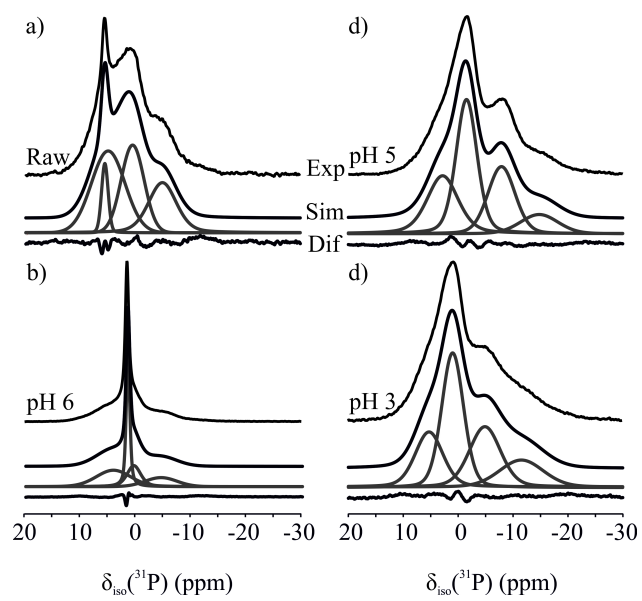


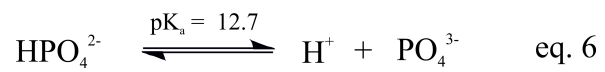
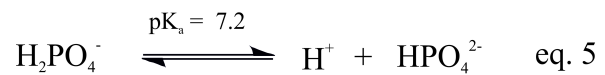
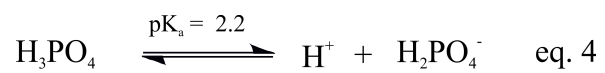












ACCEPTED MANUSCRIPT

- Up to 75 % P is released from digested sludge by acidification
- Phosphate primarily binds to the ZnAl LDH at pH = 3, 4, 5 and 6
- Sulfate reduces phosphate binding if sulfuric acid is used for acidification
- Phosphate removal is most efficient at low pH due to less dissolved carbonate
- Solid state NMR Spectroscopy and PXRD showed preservation of LDH at all pH

ACCEPTED MANUSCRIPT

Declaration of interests

The authors declare that they have no known competing financial interests or personal relationships that could have appeared to influence the work reported in this paper.

The authors declare the following financial interests/personal relationships which may be considered as potential competing interests:

none